

# Proposal for the Quantum Simulation of the $\mathbb{CP}(2)$ Model on Optical Lattices\*

Catherine Laflamme<sup>a,b</sup>, Wynne Evans<sup>c</sup>, Marcello Dalmonte<sup>a,b</sup>, Urs Gerber<sup>d,e</sup>, Héctor Mejía-Díaz<sup>d</sup>, Wolfgang Bietenholz<sup>†d</sup>, Uwe-Jens Wiese<sup>c</sup> and Peter Zoller<sup>a,b</sup>

<sup>a</sup> *Institute for Theoretical Physics, University of Innsbruck, A-6020, Innsbruck, Austria*

<sup>b</sup> *Institute for Quantum Optics and Quantum Information  
Austrian Academy of Sciences, A-6020 Innsbruck, Austria*

<sup>c</sup> *Albert Einstein Center for Fundamental Physics, Institute for Theoretical Physics  
Universität Bern, Sidlerstrasse 5, CH-3012 Bern, Switzerland*

<sup>d</sup> *Instituto de Ciencias Nucleares, Universidad Nacional Autónoma de México  
A.P. 70-543, C.P. 04510 Distrito Federal, Mexico*

<sup>e</sup> *Instituto de Física y Matemáticas, Universidad Michoacana de San Nicolás de Hidalgo  
Edificio C-3, Apdo. Postal 2-82, C.P. 58040, Morelia, Michoacán, Mexico*

E-mail: wolbi@nucleares.unam.mx

The 2d  $\mathbb{CP}(N-1)$  models share a number of features with QCD, like asymptotic freedom, a dynamically generated mass gap and topological sectors. They have been formulated and analysed successfully in the framework of the so-called D-theory, which provides a smooth access to the continuum limit. In that framework, we propose an experimental set-up for the quantum simulation of the  $\mathbb{CP}(2)$  model. It is based on ultra-cold Alkaline-Earth Atoms (AEAs) located on the sites of an optical lattice, where the nuclear spins represent the relevant degrees of freedom. We present numerical results for the correlation length and for the real time decay of a false vacuum, to be compared with such a future experiment. The latter could also enable the exploration of  $\theta$ -vacua and of the phase diagram at finite chemical potentials, since it does not suffer from any sign problem.

*The 33rd International Symposium on Lattice Field Theory  
14 -18 July 2015  
Kobe International Conference Center, Kobe, Japan*

\*We are indebted to D. Banerjee, L. Fallani, C.V. Kraus, M. Punk, E. Rico and S. Sachdev for helpful communication. This work was supported by the Schweizerischer Nationalfonds, the European Research Council by means of the European Union's Seventh Framework Programme (FP7/2007-2013)/ERC grant agreement 339220, the Mexican Consejo Nacional de Ciencia y Tecnología (CONACYT) through projects CB-2010/155905 and CB-2013/222812, and by DGAPA-UNAM, grant IN107915. Work in Innsbruck is partially supported by the ERC Synergy Grant UQUAM, SIQS, and the SFB FoQuS (FWF Project No. F4016-N23). C.L. was partially supported by NSERC.

<sup>†</sup>Speaker.

## 1. Motivation

Lattice simulations of models in quantum field theory employing a *quantum system* — *i.e.* analog quantum computing — could overcome the notorious sign problem that usually occurs if the Euclidean action is complex; in this approach, the phase factor is naturally incorporated (for recent reviews, see Refs. [1]). A prominent long-term goal of this concept is the exploration of the QCD phase diagram at finite baryon density, or a finite vacuum angle  $\theta$ . In fact, within the Standard Model of particle physics, this is one of the major issues that remain mysterious; so far, the sign problem has prevented reliable numerical studies.

As a step towards that goal, we present a proposal for the quantum simulation of the 2d  $\mathbb{CP}(2)$  model, by means of ultra-cold Alkaline Earth Atoms (AEAs) trapped in an optical lattice. Unlike previous suggestions for quantum simulations of lattice field theory, our proposal involves an automatic extrapolation to the continuum limit, taking advantage of asymptotic freedom.

## 2. $\mathbb{CP}(N-1)$ models

The 2d  $\mathbb{CP}(N-1)$  models [2] are popular toy models for QCD. They can be considered as complex analogues of the  $O(N)$  spin models, with a covariant derivative, as we see from the action in a continuous Euclidean plane,

$$S[\vec{z}] = \int d^2x (D_\mu \vec{z})^\dagger \cdot D_\mu \vec{z} - i\theta Q[\vec{z}], \quad \vec{z}(x) \in \mathbb{C}^N, \quad |\vec{z}(x)| = 1, \quad D_\mu = \partial_\mu + \frac{1}{2}(\partial_\mu \vec{z}^\dagger \cdot \vec{z} - \vec{z}^\dagger \cdot \partial_\mu \vec{z}), \quad (2.1)$$

where  $Q \in \mathbb{Z}$  is the topological charge, and  $N = 2, 3, 4, \dots$

As a remarkable property, there is a local  $U(1)$  symmetry, in addition to the global  $SU(N)$  symmetry. In an alternative notation, we can write the fields as  $N \times N$  Hermitian projection matrices,

$$P(x) = |\vec{z}(x)\rangle\langle\vec{z}(x)|, \quad \text{Tr} P(x) = 1, \quad P(x) = P(x)^2 = P(x)^\dagger. \quad (2.2)$$

The case  $N = 2$  corresponds to the  $O(3)$  model. For higher  $N$ , all 2d  $\mathbb{CP}(N-1)$  models have topological sectors too (in contrast to the higher 2d  $O(N)$  models). Therefore it is natural to include a  $\theta$ -term, as it has been done in eq. (2.1). As further properties in common with QCD, all the 2d  $\mathbb{CP}(N-1)$  models are asymptotically free, and they display a dynamically generated mass gap.

### 2.1 D-theory formulation

In D-theory, asymptotically free models are formulated in a space with an additional dimension; in the weak coupling extrapolation towards the continuum limit, this additional direction is suppressed by dimensional reduction [3].

In particular, the D-theory formulation of 2d  $\mathbb{CP}(N-1)$  models starts with 2d layers, where  $SU(N)$  quantum spins are located on a “ladder”, *i.e.* on a  $L \times L'$  lattice with  $L \gg L'$  [4]. Hence each layer contains a set of  $L'$  long quantum spin chains. These layers are embedded in a 3d space, which includes an additional  $\beta$ -direction. The Hamiltonian can be written as

$$H = -J \sum_{\langle xy \rangle} \sum_{a=1}^{N^2-1} T_x^a T_y^{a*}, \quad (2.3)$$

where  $T_x^a$  ( $T_y^{a*}$ ) are spin operators in the (anti-)fundamental representation of  $SU(N)$ , such that  $[T_x^a, T_y^b] = i\delta_{xy}f^{abc}T_x^c$  (with the  $SU(N)$  structure constants  $f^{abc}$ ). Here we deal with a positive coupling constant,  $J > 0$ , which corresponds to an anti-ferromagnetic system.

For  $N = 3$  and 4, Ref. [5] pointed out that (in the limit of zero temperature and infinite volume) this system undergoes spontaneous symmetry breaking  $SU(N) \rightarrow U(N-1)$ , which generates  $2(N-1)$  Nambu-Goldstone bosons. They are accommodated in the coset space of the *complex projection*,  $\mathbb{CP}(N-1) = SU(N)/U(N-1)$ , such that the low energy effective description coincides with the  $\mathbb{CP}(N-1)$  model.

In the notation (2.2), the D-theory continuum action takes the form

$$S[P] = \frac{1}{g^2} \int_0^\beta dx_3 \int d^2x \text{Tr} \left[ \sum_{i=1}^2 \partial_i P \partial_i P + \frac{1}{c^2} \partial_3 P \partial_3 P \right] - i\theta Q[P],$$

$$i\theta Q[P] = \frac{1}{\pi} \int_0^\beta dx_3 \int d^2x \text{Tr} [P \partial_1 P \partial_3 P], \quad g^2 = \frac{c}{\rho_s L'}, \quad (2.4)$$

where  $c$  is the spin wave velocity, and  $\rho_s$  the spin stiffness.

If we return to a finite  $L \times L'$  lattice on the spatial layers, asymptotic freedom implies that the (spatial) correlation length  $\xi$  (the inverse mass of the quasi Nambu-Goldstone bosons) diverges exponentially when  $L'$  becomes large,

$$\xi \propto e^{\text{const.} \cdot L'}, \quad (2.5)$$

where we assume  $L' \ll L, \beta$ . This divergence leads to dimensional reduction; ironically, as  $L'$  grows, it becomes negligible, since  $\xi \gg L'$ . Thus we recover the 2d  $\mathbb{CP}(2)$  or  $\mathbb{CP}(3)$  model, with  $\theta = L'\pi$  [4] (since the integrand of the expression for  $Q[P]$  is constant in  $x_2$ ).

In view of the prospects to implement the  $SU(N)$  quantum spin system experimentally [6], to be discussed in the next section, it is important to explore this exponential growth explicitly. Figure

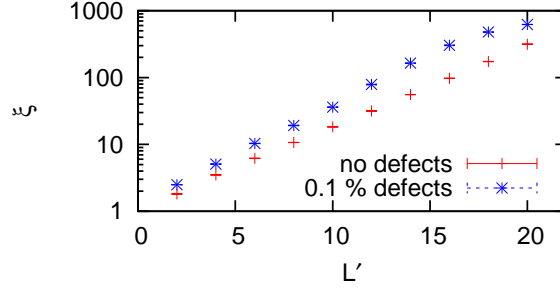


**Figure 1:** The correlation length  $\xi$  as a function of  $L'$ , for an  $SU(3)$  quantum spin model on a  $\beta \times L \times L'$  lattice, at  $L = 1500$  and  $\beta J = 1000$ . The red crosses (blue asterisks) refer to the setting when all sites are occupied (with 0.1% of random distributed empty sites). Error bars are included, but hardly visible. The results for  $\xi$  and for the second moment correlation length  $\xi_2$  agree up to tiny differences, which are not visible either. With or without defect sites,  $\xi$  grows exponentially in  $L'$ , which confirms eq. (2.5) and therefore asymptotic freedom; we further see that a moderate  $L' \approx 10$  is sufficient for dimensional reduction.

1 shows simulation results, which were obtained with a loop cluster algorithm [7] at  $L = 1500$  and  $\beta J = 1000$ . The boundary conditions are open in the (short)  $L'$ -direction, as in the experiment, and periodic in the long directions (where it hardly matters). We obtain  $\text{const.} = 0.270784$ , and observe that  $L' \approx 10$  is sufficient for the dimensional reduction to set in, essentially. In fact, such a number of coupled quantum spin chains is experimentally realistic.

In an experiment it may happen that a few sites in the optical lattice remain unoccupied. Frequent repetition of this experiment restores translation invariance statistically, but the correlation length is enhanced. Numerical data for this setting, with 0.1% of such defect sites are also shown in Figure 1. Again there is clear evidence that  $\xi$  grows exponentially in  $L'$  (as long as finite size effects are small), in accordance with relation (2.5), which reflects asymptotic freedom. Dimensional reduction sets in even earlier in this case.

### 3. Experimental set-up

The goal is to implement the Hamiltonian (2.3) by ultra-cold fermionic AEAs on the sites of an optical lattice. The latter is formed by the nodes of superimposed standing laser waves, as sketched in Figure 2, with a spacing in the  $\mu\text{m}$  magnitude. The temperature is of the order of nK, which

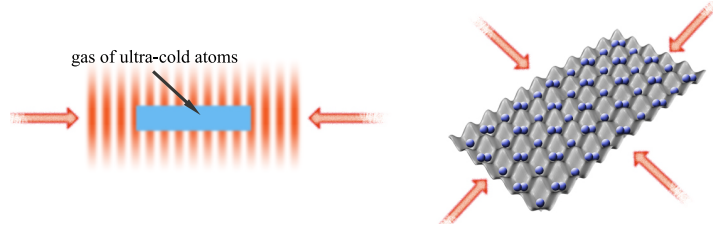


**Figure 2:** Illustration of optical lattices, where the sites correspond to the nodes of standing laser waves.

keeps the atoms in their electronic ground state. For fermionic AEAs, the electron and nuclear spins decouple almost completely in the ground state manifold, which excludes spin changing collisions. Moreover, in an external magnetic field, the interactions between the Zeeman states are  $SU(N)$  symmetric, where  $N \leq 2I + 1$  and  $I$  is the nuclear spin [8], and the total spin is conserved. This can be implemented up to  $N = 10$ , e.g. with  $^{87}\text{Sr}$  atoms [8].

Next we re-write the spin operators in terms of fermionic bilinears, composed of  $d_x$  and  $d_x^\dagger$ ,

$$T_x^a = d_{xm}^\dagger \lambda_{mm'}^a d_{xm'}, \quad -T_x^{a*} = -d_{xm}^\dagger \lambda_{mm'}^{a*} d_{xm'}, \quad (3.1)$$

where  $m, m' = 1 \dots N$  label the states, and  $\lambda^a$  are generalised Gell-Mann matrices,  $\text{Tr}[\lambda^a, \lambda^b] = \delta^{ab}$ . Now the Hamiltonian is split into a hopping term and a potential,

$$H = H_t + H_U, \quad H_t = -t \sum_{\langle xy \rangle, m} \left( c_{xm}^\dagger c_{ym} + c_{ym}^\dagger c_{xm} \right), \quad H_U = \frac{U}{2} \sum_x n_x (n_x - 1) + V \sum_{x \in A} n_x, \quad (3.2)$$

where the operator  $c_{xm}$  annihilates the nuclear spin level  $m \in \{-I \dots I\}$  at site  $x$ ,  $t$  is the hopping parameter,  $U$  the on-site interaction,  $n_x = \sum_m c_{xm}^\dagger c_{xm}$  the occupation number, and  $V$  is the energy offset between two staggered sub-lattices, which we denote as  $A$  and  $B$ . This system is illustrated in Figure 3, and the caption explains the relation between the operators  $c_{xm}$  and  $d_{xm}$ . The initial state should be prepared with one AEA on each site of sub-lattice  $A$ , which corresponds to one fermion; on each site of sub-lattice  $B$  there are  $N - 1$  AEAs, corresponding to  $N - 1$  fermions, or one hole.

The hopping parameter  $t$  fixes the coupling constant  $J$ , to be tuned by varying the energy offset  $V$ . At strong coupling,  $t \ll U, V$ , the system is essentially in the eigenstates of  $H_U$ , with virtual tunnelling due to the  $SU(N)$  exchange terms in  $H_t$ . A hopping parameter expansion up to  $O((t/U)^2)$  reproduces the form of  $H$  in eq. (2.3) [9], with

$$J = \frac{t^2 U}{[-V + U(N - 3)][V - U(N - 1)]}. \quad (3.3)$$

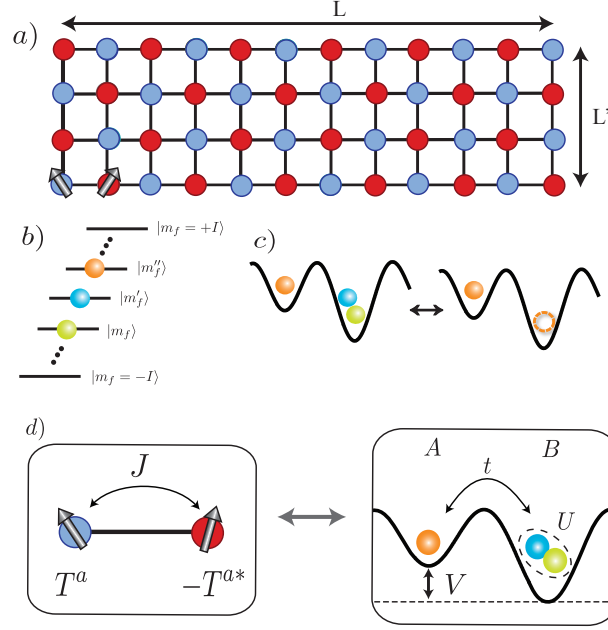


**Figure 3:** An illustration of the experimental set-up: a)  $SU(N)$  spins on a bipartite  $L' \times L$  lattice,  $L \gg L'$ . b) The  $N \leq 2I + 1$  hyperfine states of an AEA, in an external magnetic field which induces Zeeman splitting. c) On sub-lattice  $A$  the  $SU(N)$  quantum spins are in the fundamental representation, and we identify  $c_x = d_x^\dagger$ . On sub-lattice  $B$  they are in the anti-fundamental representation, and  $c_x = d_x$ . Hence the exchange of the staggered sub-lattices  $A \leftrightarrow B$  corresponds to a particle-hole transformation. d) The nearest-neighbour interactions between  $T_{x \in A}^a$  and  $-T_{y \in B}^{a*}$ .

The preparation of the initial state proceeds as follows: first one fills each site with  $N$  AEAs, where each level  $m$  is occupied once<sup>1</sup> (this can be achieved by optical pumping [10]). Then each site is split adiabatically into a double-well, forming the sub-lattices  $A$  and  $B$ , cf. Figure 3. The barrier is tuned to match the quantum dynamics according to the Hamiltonian  $H$ ; this has already been realized for bosonic alkaline atoms [11]. Based on experimental experience, we expect this to be feasible up to large  $L = O(1000)$  and  $L' \approx 12$ ; according to our results in Figure 1, this is sufficient for dimensional reduction to set in. The results for the correlation length  $\xi$  can be confronted with experimental measurements by means of Bragg spectroscopy or noise correlation [12].

#### 4. Phase transition at $\theta = \pi$ and false vacuum decay

An odd number  $L'$  implies  $\theta = \pi$ , where a first order phase transition and the spontaneous breaking of the  $C$  (charge conjugation) symmetry is expected [13]; Refs. [4] provide numerical evidence for this scenario.

In the experiment, a  $C$  transformation corresponds to a shift in the  $L$ -direction by one lattice spacing. If  $x$  ( $x + \hat{1}$ ) belongs to sub-lattice  $A$  ( $B$ ), then this shift transforms  $T_x^a \rightarrow -T_{x+\hat{1}}^{a*}$ , and  $-T_x^a \rightarrow T_{x+\hat{1}}^{a*}$ . The order parameter for  $C$  symmetry [14],

$$D = \sum_{x \in A} \langle T_x^a T_{x+\hat{1}}^{a*} - T_x^a T_{x-\hat{1}}^{a*} \rangle, \quad (4.1)$$

<sup>1</sup>A non-uniform occupation of the Zeeman states may also be intended, since it captures the  $\mathbb{CP}(N-1)$  model at finite density.

detects *dimerisation*. At  $\theta = 0$ , C invariance holds, and  $D = 0$ . It breaks at  $\theta = \pi$ , where there are two degenerate ground states with  $\pm D$ , which we denote as  $|\pm\rangle$ . These ground states may be distinguished by bonds between nearest-neighbour sites, which can be set in two ways, as shown in Figure 4. For ultra-cold atoms, the singlets that contribute to  $D$  can be measured by spin changing collisions [12, 15].

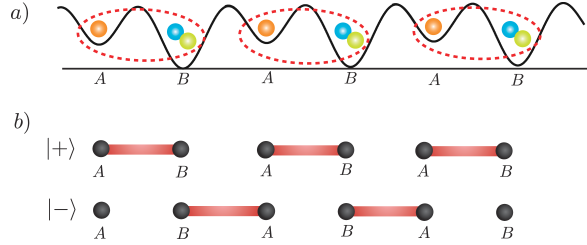


**Figure 4:** An illustration of the two degenerate ground states at  $\theta = \pi$ . In this case, there is dimerisation (in an ambiguous way), and C symmetry is broken.

At last we consider a dynamical process for a single spin chain of even length  $L$ : starting from total dimerisation, one turns on the hopping parameter  $t$  adiabatically. We describe the gradual modification by a parameter  $\tau$ , which increases from 0 to 1, such that the dynamics is driven by the Hamiltonian

$$H(\tau) = \tau H - (1 - \tau) J \sum_{x \in A} T_x^a T_{x+1}^{a*}. \quad (4.2)$$

Numerical results for the evolution of the first two energy eigenvalues,  $E_0$  and  $E_1$ , are shown in Figure 5 on the left. Their evaluation also reveals the time dependent dimerisation  $D(t)$ . The latter is shown in the right panel of Figure 5, along with a dimerisation map in the state  $|-\rangle$ . The evolution turns it into a false vacuum, which performs an (incomplete) decay towards the true vacuum  $|+\rangle$ , such that  $D(t)$  decreases in an oscillatory manner. For a similar study of the real time dynamics of coupled bosonic spin chains, we refer to Ref. [16].

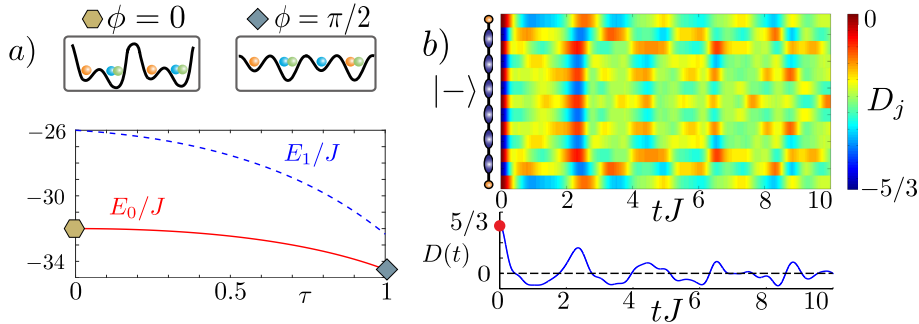


**Figure 5:** The time evolution of the first two energy eigenvalues,  $E_0/J$  and  $E_1/J$  (on the left), and of the dimerisation  $D(t)$  (on the right), if one starts from total dimerisation and switches on the hopping parameter  $t$  adiabatically. Then the Hamiltonian (4.2) drives the dynamics, turning the initial vacuum state  $|-\rangle$  into a false vacuum, which decays such that  $D(t)$  decreases and oscillates, as shown on the right.

This time evolution has been computed by the exact diagonalisation of  $H(\tau)$  at  $L = 14$ . It corresponds to the real time evolution of a false vacuum in the  $\mathbb{CP}(2)$  model, which cannot be obtained with classical Monte Carlo simulations, due to the sign problem. The experimental set-up described here should enable a quantum simulation, which can be compared to the results in Figure 5, and which can be extended to large  $L$ .

## 5. Summary

We have described a proposal for the quantum simulation of  $\mathbb{CP}(N - 1)$  models by ultracold AEAs trapped in an optical lattice. They represent a model of  $SU(N)$  quantum spins, with  $N \leq 2I + 1$ , where  $I$  is the nuclear spin. This system corresponds to the 3d D-theory formulation of the  $\mathbb{CP}(N - 1)$  model, where dimensional reduction leads directly to the continuum limit of the 2d model, thanks to asymptotic freedom. Our results for the correlation length at  $N = 3$  show that for a realistic system size, dimensional reduction leads to the 2d continuum  $\mathbb{CP}(2)$  model.

Experimental tools for the ground state preparation in such systems, and also for its adiabatic modification, do already exist [8, 10–12, 15]. We discussed the dynamics of C symmetry restoration, which corresponds to a real time evolution in the  $\mathbb{CP}(2)$  model. For small systems it was evaluated by the diagonalisation of the Hamiltonian; for larger systems it can be measured by the experiment, which acts as an analog quantum computer.

## References

- [1] U.-J. Wiese, *Annalen Phys.* 525 (2013) 777.  
E. Zohar, J.I. Cirac and B. Reznik, arXiv:1503.02312 [quant-ph]
- [2] A. D’Adda, M. Lüscher and P. Di Vecchia, *Nucl. Phys.* B146 (1978) 63.
- [3] S. Chandrasekharan and U.-J. Wiese, *Nucl. Phys.* B492 (1997) 455.  
R. Brower, S. Chandrasekharan and U.-J. Wiese, *Phys. Rev.* D60 (1999) 094502.  
R. Brower, S. Chandrasekharan, S. Riederer and U.-J. Wiese, *Nucl. Phys.* B693 (2004) 149.
- [4] B.B. Beard, M. Pepe, S. Riederer and U.-J. Wiese, *Phys. Rev. Lett.* 94 (2005) 010603.  
S. Riederer, Ph.D. thesis, Universität Bern, 2006.
- [5] K. Harada, N. Kawashima and M. Troyer, *Phys. Rev. Lett.* 90 (2003) 117203.
- [6] C. Laflamme *et al.*, arXiv:1507.06788 [quant-ph].
- [7] H.G. Evertz, G. Lana and M. Marcu, *Phys. Rev. Lett.* 70 (1993) 875.  
U.-J. Wiese and H.-P. Ying, *Z. Phys.* B93 (1994) 147.
- [8] A.V. Gorshkov *et al.*, *Nature Phys.* 6 (2010) 289.
- [9] A. Auerbach, *Interacting Electrons and Quantum Magnetism* (Springer, 1994).
- [10] G. Pagano *et al.*, *Nature Phys.* 10 (2014) 198. F. Scazza *et al.*, *Nature Phys.* 10 (2014) 779.
- [11] S. Nascimbène *et al.*, *Phys. Rev. Lett.* 108 (2012) 205301.
- [12] I. Bloch, J. Dalibard and S. Nascimbène, *Nature Phys.* 8 (2012) 267.
- [13] N. Seiberg, *Phys. Rev. Lett.* 53 (1984) 637.
- [14] N. Read and S. Sachdev, *Phys. Rev. Lett.* 62 (1989) 1694.
- [15] B. Paredes and I. Bloch, *Phys. Rev.* A77 (2008) 023603.
- [16] S.F. Caballero-Benítez and R. Paredes, *Phys. Rev.* A85 (2012) 023605.